

## A Class of Stabilizing PID Controllers for Position Control of Single-Link Robot

<sup>1</sup>Leena G., <sup>2</sup>K. B. Datta, <sup>2</sup>G. Ray

<sup>1</sup>*Professor, Electrical and Electronics Engineering, Manav Rachna International University, Faridabad, Haryana, 121001, India –Corresponding author  
leenagjeevan@rediffmail.com*

<sup>2</sup>*Department of Electrical Engineering, Indian Institute of Technology, Kharagpur, West Bengal 721302, India  
attadbitnak@yahoo.com, gray@ee.iitkgp.ernet.in*

### Abstract

*A class of stabilizing proportional-integral-derivative (PID) controllers for a nonlinear system is designed using different techniques. The ranges of controller parameters are obtained by a search technique (1) checking the stability of the system by solving an interval Lyapunov equation, (2) checking the quadratic stability, (3) checking the stability of the system by solving Lyapunov equation, (4) solving stability boundary equations.. This characterization is useful for designing an optimal set of controller parameters. A simulation example of a single-link robot manipulator is considered to demonstrate the applicability of the proposed control schemes.*

**Key words:** *Lyapunov equation, boundary equation, interval matrix, quadratic stability, robot manipulator*

### 1. Introduction

A class of all stabilizing P, PI and PID controllers was designed by Bhattacharya et al [1] using generalized Hermite Biehler theorem. This characterization of all feedback gain values is useful for carrying out optimal designs with respect to various performance indices. Most of the industrial controllers even today are either proportional- integral (PI) or proportional-integral-derivative (PID) types [13] and hence the result of the above paper had great significance. One of the drawbacks of the above design method is that it can be applied only to linear system. Moreover, it has been a long standing belief that PID control is inadequate to cope with highly nonlinear system, since the design of the control law is based solely on linear models. A very important technology is necessary to introduce for industrial robot to realize a fine and fast positioning control. Most of the robots employed in industry are often equipped with conventional PID controllers due to their simplicity in structure and ease of design. In practice, a simple linear PID feedback controller with appropriate control gains may lead to the desired position without causing any steady-state error. This is the reason why PID controllers are still used in industrial robots. In true sense, however, PID controller does not ensure to achieve a desired level of control performance, while dynamic equations for mechanical manipulators are highly uncertain due to load changes and nonlinear friction effects.

In this paper, a class of stabilizing controllers for a single-link robot was found out using a simple design technique where the feedback gains are obtained by checking the stability of the closed-loop system. Subsequently we obtain the range of PID controllers for the single-link robot manipulator and it is discussed in detail.

This paper is organized as follows. In Section 2, we describe the dynamic model of a single-link manipulator. In Section 3, we obtain the complete characterization of all stabilizing PID controllers for a single-link manipulator using different methods. In Section 4, a simulation example is given to demonstrate the applicability of the proposed control schemes. An optimal selection of PID controller parameter for each method based on genetic algorithm is obtained from the stabilizing region of controller parameters and it is discussed in the same section. Finally, the conclusions are included in section 5.

## 2. Dynamic Model of a Robot and Problem Formulation

The dynamic equation of a single-link robot manipulator shown in Fig. 1, is described by [2]

$$\tau = J_m \ddot{\theta} + f(\dot{\theta}) + ml g \cos \theta \quad (1)$$

where  $\theta$  is the link angle,  $m$  and  $J_m$  are the mass and the rotational inertia of the link, respectively,  $l$  is the distance from the joint axis to the link center mass,  $f$  is the friction function, and  $\tau$  is the output torque of motor reflected to the joint axis. If the link is modeled as a point mass at the distal end,  $J_m = ml^2$ .

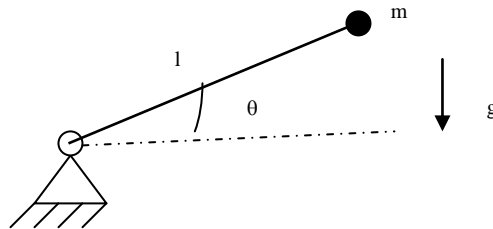


**Fig.1 Schematic of one link revolute robot**

Let  $\theta_d$  denote the desired constant joint position and  $\theta(0), \dot{\theta}(0)$  be any given initial condition. The classical PID control law can be written as

$$\tau = K_p e(t) + K_d \dot{e}(t) + K_i \int_0^t e(t) dt \quad (2)$$

where  $e(t) = \theta_d - \theta(t)$  is the position error,  $K_p$ ,  $K_i$  and  $K_d$  are respectively, the proportional, integral and derivative gains of the PID controller. The control problem is to provide a complete solution to the constant gain stabilizing control parameters  $K_p, K_i, K_d$  such that the position error  $e(t)$  vanishes with time, i.e.  $\lim_{t \rightarrow \infty} e(t) = 0$ .

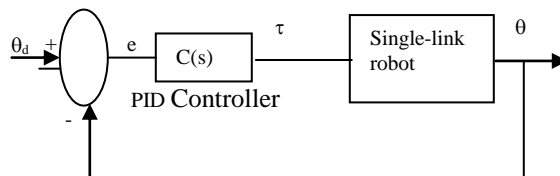


**Fig. 2 Block diagram of single robot system**

### 3. Design of all Stabilizing PID Controller Gains

Let us consider the feedback system shown in Fig.2 where  $\theta_d$  is the desired command signal and  $\theta$  is output. Now combining the dynamics of single-link robot acting in a friction free space ( $f(\theta) = 0$ ) and control law (equations 1 & 2) we obtain

$$J_m \ddot{e}(t) + K_d \dot{e}(t) + [K_p - ml g \sin(\theta_d - e(t))]e(t) + K_i e(t) = 0 \quad (3)$$

Then the following state space form can represent the above error system dynamic equation

$$\dot{X} = \begin{bmatrix} 0 & 1 & 0 \\ 0 & 0 & 1 \\ -K_i / J_m & -(K_p - ml g \sin \theta) / J_m & -K_d / J_m \end{bmatrix} X(t) \quad (4)$$

where  $x_1(t) = e(t)$ ,  $x_2(t) = \dot{e}(t)$  and  $x_3(t) = \ddot{e}$

In this paper we will consider the different design techniques for characterization of all stabilizing PID controllers.

#### 3.1 Method 1: Based on interval matrix approach

It may be noted that the system equation (4) can now be changed to an interval matrix by assigning the value of  $\sin(\theta_d - x_1)$  in the range of [0 1] and more specifically the position of robot link can be placed any location in the range  $\theta (= \theta_d - x_1) = 0$  to  $180^\circ$ . Furthermore the system matrix given in equation (4) thus becomes an interval matrix as

$$\begin{aligned} \dot{X}(t) &= \begin{bmatrix} 0 & 1 & 0 \\ 0 & 0 & 1 \\ -K_i / J_m & 1/J_m[-K_p & -K_p + ml g] & -K_d / J_m \end{bmatrix} X(t) \\ &= A_I X(t) = [A_C - \Delta, A_C + \Delta] X(t) \end{aligned} \quad (5)$$

where  $A_C$  is the center or nominal matrix and  $\Delta$  is the perturbed matrix. In order to check the stability of the interval matrix  $A_I$  we use the result of Garofalo et al [3]-[5]. It is assumed that the nominal matrix  $A_C$  is asymptotically stable for the choice of PID controller parameters. An equivalent statement is that for any symmetric positive definite matrix  $Q_0$  there exists a unique symmetric positive definite matrix  $P_0$  [3] such that

$$A_C^T P_0 + P_0 A_C = -Q_0 \quad (6)$$

We focus our attention on the stability of the interval system (5) and this can be achieved by considering the same  $P_0$  matrix as obtained from equation (6). This means that we could check the positive definiteness of the interval matrix

$$Q_I = -(A_I^T P_0 + P_0 A_I) \quad (7)$$

In general, it is difficult to check the positive definiteness of an interval matrix  $Q_I$ , but the structure of the matrix  $A_I$  can help in solving the equation (7) in a simpler way. Since the matrix  $A_I$  is an interval matrix, each entry of it is a continuous function over a compact set,

with its maximum and minimum range. For this class of matrices, a sufficient condition for matrix  $Q_I$  defined by (7) to be positive definite [5] is that the matrices

$$Q^r = -(A^r)^T P_0 + P_0 A^r \quad (8)$$

be positive definite for all  $r = 1, 2, \dots, 2^{n^2}$ , where  $n$  is the number of elements in  $A$  having interval range (for the present case,  $n = 1$  and  $r = 1, 2$ ). The matrix  $A^r$  is the corner matrices of  $A_I$  and more specifically

$$A^1 = \begin{bmatrix} 0 & 1 & 0 \\ 0 & 0 & 1 \\ -K_i & -K_p & -K_d \end{bmatrix} \text{ and } A^2 = \begin{bmatrix} 0 & 1 & 0 \\ 0 & 0 & 1 \\ -K_i & -K_p + ml g & -K_d \end{bmatrix}$$

In the proposed method we search for the range of PID controller parameters by checking the positive definiteness of  $Q^1$  and  $Q^2$  after solving  $P_0$  [5] from the Lyapunov equation (6). The algorithmic steps involved to obtain the range of controller parameters are given in Appendix I and explained through flow diagram in fig. 20.

### 3.2 Method 2: Based on quadratic stability approach

The investigation of stability domains for state space models has been addressed in many papers during the last decades. The use of Lyapunov functions [14-17] is certainly the main approach for this kind of analysis, since bounds for the stability domains can be found in terms of the associated Lyapunov matrix and the allowed perturbation direction. For linear systems with uncertain parameters, a polytopic bounding approach was proposed in literature and the quadratic stability conditions over the entire uncertainty polytope have been derived. The results of quadratic stability conditions are conservative and many attempts have been made to reduce the conservatism by seeking parameter dependent techniques for determining the stability of system with polytopic type uncertainties. These techniques assign a Lyapunov function to each vertex of the uncertainty polytope and subsequently parameter dependent condition for the stability of linear systems with polytopic uncertainty has been introduced in [6] - [7]. It is worth of mentioning that the stability domains can be computed by evaluating all the vertices of the polytope.

The dynamic equation of the system (4) is a function of  $\theta$  ( $e = x_1 = \theta_d - \theta$ ) and it can be considered an uncertain time-varying system since  $\theta$  is varying with respect to time. A time-varying system can be modeled as a polytopic system and this model is also called Polytopic Linear Differential Inclusions (PLDI) in the literature and it is given in Appendix II.

Consider the system (4) and the corresponding polytopic system is quadratically stable if and only if [6] there exists a common Lyapunov matrix  $P > 0$  such that

$$A_i^T P + P A_i < 0 \quad i = 1, 2, \dots \quad (9)$$

where the system matrix of equation (4) ranges in the polytope by its vertices.

$$A_1 = \begin{bmatrix} 0 & 1 & 0 \\ 0 & 0 & 1 \\ -K_i & -K_p & -K_d \end{bmatrix}, \quad A_2 = \begin{bmatrix} 0 & 1 & 0 \\ 0 & 0 & 1 \\ -K_i & -K_p + ml g & -K_d \end{bmatrix};$$

Each vertex is computed by taking alternatively the maximum and minimum values of each element of the system matrix of equation (4). We can find out the range of controller parameters by checking the quadratic stability of PLDI system using the MATLAB LMI Control Toolbox [8] and simultaneously adopting the procedure given in Appendix I.

### 3.3 Method 3: Based on Lyapunov function

The necessary conditions for stability of the closed-loop system (4) are given by the following expressions.

$$K_i > 0, \quad K_d > 0 \quad \text{and} \quad K_p > ml g \sin \theta \quad (10)$$

In order to study the stability of the system (4) we introduce the Lyapunov function

$$V(X(t), t) = X^T(t)PX(t) \quad (11)$$

where  $P = (p_{ij})$  is a positive definite matrix and the diagonal elements of  $P$  are nonzero and positive (i.e.  $p_{ii} > 0, i = 1, 2, 3$ ). The time derivative of  $V$  along the trajectories of (4) is given by

$$\dot{V} = \frac{\partial V}{\partial t} = \frac{\partial V}{\partial X} \dot{X} \quad (12)$$

The above equation is now written in explicit form as

$$\begin{aligned} \dot{V}(X(t), t) = & -2p_{13}K_i / J_m x_1^2 + 2(p_{12} + p_{23}(-K_p + ml g \sin \theta) / J_m)x_2^2 + 2(p_{23} - p_{33}K_d / J_m)x_3^2 \\ & + 2(p_{11} + p_{13}(-K_p + ml g \sin \theta) / J_m - p_{23}K_i / J_m)x_1x_2 + 2(p_{12} - p_{33}K_i / J_m - p_{13}K_d / J_m)x_1x_3 \\ & + 2(p_{22} + p_{13} - p_{23}K_d / J_m + p_{33}(-K_p + ml g \sin \theta) / J_m)x_2x_3. \\ \leq & -2p_{13}K_i / J_m x_1^2 + 2(p_{12} + p_{23}(-K_p + ml g \sin \theta) / J_m)x_2^2 + 2(p_{23} - p_{33}K_d / J_m)x_3^2 + \\ & (p_{11} + p_{13}(-K_p + ml g \sin \theta) / J_m - p_{23}K_i / J_m)(x_1^2 + x_2^2) + (p_{12} - p_{33}K_i / J_m - p_{13}K_d / J_m)(x_1^2 + x_3^2) \\ & + (p_{22} + p_{13} - p_{23}K_d / J_m + p_{33}(-K_p + ml g \sin \theta) / J_m)(x_2^2 + x_3^2), \text{ since} \\ & x_i^2 + x_j^2 \geq 2x_ix_j \end{aligned} \quad (13)$$

It can be noted that the sign of the cross product terms  $x_ix_j$  are indefinite and the coefficients associated with these terms are assigned to zero to satisfy  $\dot{V}(X(t), t) < 0$ . This in turn, needs to satisfy the following six equations.

$$-p_{13}K_i / J_m < 0 \quad (14)$$

$$p_{12} + p_{23}(-K_p + ml g \sin \theta) / J_m < 0 \quad (15)$$

$$p_{23} - p_{33}K_d / J_m < 0 \quad (16)$$

$$p_{11} + p_{13}(-K_p + ml g \sin \theta) / J_m - p_{23}K_i / J_m = 0 \quad (17)$$

$$p_{12} - p_{33}K_i / J_m - p_{13}K_d / J_m = 0 \quad (18)$$

$$p_{22} + p_{13} - p_{23}K_d / J_m + p_{33}(-K_p + ml g \sin \theta) / J_m = 0 \quad (19)$$

Using the equation (10) and the properties of  $P > 0$  ( $p_{ii} > 0$ ,  $i = 1, 2, 3$ ) in equations (12) - (19), one can easily arrive at the following necessary conditions by carefully examining the equations (12) - (19).

$$p_{13} > 0, \quad p_{12} > 0 \quad \text{and} \quad p_{23} > 0$$

Equations (14) – (19) are solved for wide choice of controller parameters ( $K_p, K_i, K_d$ ) with  $\theta = 90^\circ$  in order to achieve not only  $\dot{V}(X(t), t) < 0$ , but also to satisfy  $P > 0$ .

It can be noted further from the equations (14)- (19) that the same value of  $P$  and the controller parameters that are obtained in previous step for  $\theta = 90^\circ$  can also be used in equations (14)- (19) for  $0 < \theta < 180^\circ$  to ensure  $\dot{V}(X(t), t) < 0$ . Equations (14)-(19) implies that the controller designed parameters for  $\theta = 90^\circ$  will stabilize a family of plants while the desired position of the robot arm angle  $\theta$  varies from  $\theta = 0^\circ$  to  $\theta = 180^\circ$ .

### 3.4 Method 4: Based on stability boundary equation

The concepts of gain margin and phase margin of single input single output (SISO) systems are well defined and understood. They reflect on the performance and stability of the system and widely used for controller designs. A classical approach to consider model uncertainties is to design the closed-loop control system with sufficient gain and phase margins and it is then guaranteed that gain variation and phase delays do not lead to instability. A class of research workers has extended these SISO phase and gain margin concepts to multivariable systems and it can be found in literature [18-20].

The concept of stability equation method [9] is employed to obtain stability boundary of a system and simultaneously the gain margins (equal to 1) and phase margins (equal to zero) are maintained along the stability boundary in a controller parameter plane or parameter space. We recall the equation (1) and can be rewritten as

$$J_m \ddot{\theta} = \tau - ml g \cos\theta \quad (\text{assuming that the robot is acting in friction free space})$$

The block diagram representation of the above system is considered here by taking  $ml g \cos \theta$  as another input acting on the system.

Fig. 3 shows the s-domain representation of the system with a PID controller, where  $R_1(s)$  and  $R_2(s)$  are the inputs to the system,  $Y(s)$  is the output and  $\tau$  is the controller ( $C(s) = K_p + K_i/s + s K_d$ ) output acting as an input to the system.

The system output for the system under consideration is given by

$$\begin{aligned} Y(s) &= Y_1(s) + Y_2(s) \\ &= \frac{G(s)C(s)}{1 + G(s)C(s)} R_1(s) - \frac{G(s)}{1 + G(s)C(s)} R_2(s) \\ &= \frac{1}{1 + G(s)C(s)} \begin{bmatrix} G(s)C(s) & -G(s) \end{bmatrix} \begin{bmatrix} R_1(s) \\ R_2(s) \end{bmatrix} \end{aligned} \quad (20)$$

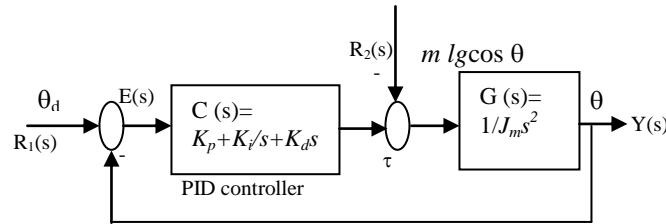


Fig 3 Another form of block diagram representation of a single-link robot

The open loop transfer function from each input ( $R_1(s)$  or  $R_2(s)$ ) to the output  $Y(s)$  can be written as

$$G_C(s) = G(s)C(s) \quad (21)$$

For  $s = j\omega$ , then we have

$$G(j\omega)C(j\omega) = \alpha e^{j\beta} \quad (22)$$

where  $|G(j\omega)C(j\omega)| = \alpha$  and  $\angle G(j\omega)C(j\omega) = \beta$

Equation (22) can be written in the following form [21]

$$1 + \frac{1}{\alpha} e^{-j(180+\beta)} G(j\omega)C(j\omega) = 0$$

$$1 + Ae^{-j\gamma} G(j\omega)C(j\omega) = 0 \quad (23)$$

where  $A = \frac{1}{\alpha} = \frac{1}{|G(j\omega)C(j\omega)|}$  and  $\gamma = 180 + \beta$

It can be noted that  $A$  is the gain margin of the system when  $\gamma = 0$  and  $\gamma$  is the phase margin when  $A=1$ . More specifically, one can easily determine the gain margin and phase margin of the system by adopting the gain-phase margin tester  $Ae^{-j\gamma}$ , which can be represented by an additional block in cascade with  $G(s)C(s)$  and shown in fig. 4

Using the expression for  $C(j\omega) = K_p + K_v/j\omega + K_d j\omega$  in eqn.(23) and evaluating the real and imaginary part to zero, we get

$$R = \text{Re}[1 + Ae^{-j\gamma} G(j\omega)C(j\omega)] = 0 \quad (24)$$

$$I = \text{Im}[1 + Ae^{-j\gamma} G(j\omega)C(j\omega)] = 0 \quad (25)$$

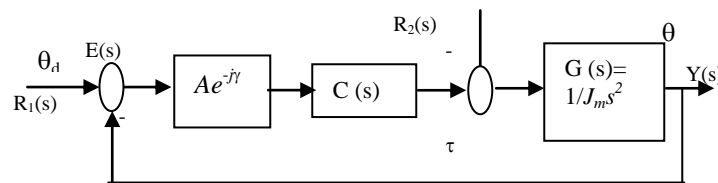


Fig. 4 Feedback control system with a gain and phase tester

It can be noted that the number of controller parameters are more than the number of equations and it is necessary to assign one of the controller parameter (say  $K_d$ ) and the remaining controller parameters are solved from equations (24) and (25). To have the stable

region in the parametric plane, one generally finds the stability boundary first, and then determines the stable region by the sign of  $J_j$  ( $J_j = \partial R / \partial K_p \cdot \partial I / \partial K_i - \partial R / \partial K_i \cdot \partial I / \partial K_p$ ). If the sign of  $J_j$  is positive (negative) facing the direction in which  $\omega$  is increasing, the left (right) side of the stability boundary is the stable region [10]. Thus one can obtain the range of controller parameters ( $K_p$ ,  $K_i$ ) for a fixed value of  $K_d$  from the boundary of the stability region.

#### 4. Simulation Results

To illustrate the proposed stabilizing control schemes, a simulation example is carried out for a one-link robot manipulator. For simplicity a single-link revolute joint robot operating in a friction-free space with point mass acting at the distal end of the link is considered. The dynamic equation of the one link robot manipulator is given by

$$\tau = ml^2 \ddot{\theta} + mlg \cos \theta$$

The parameters are set as  $m = 1.0$  kg,  $l = 1.0$  m and  $g = 9.81$  m/s<sup>2</sup>.

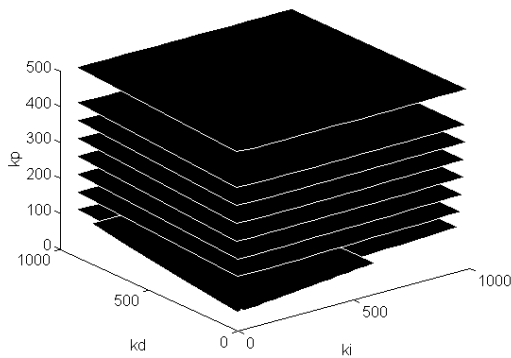


Fig. 5 The stabilizing set of ( $K_p, K_i, K_d$ ) values by method 1

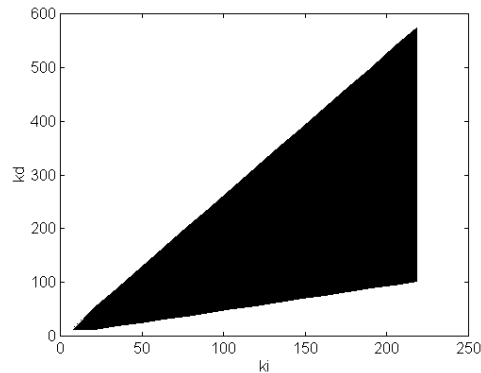


Fig. 6 The plane of ( $K_i, K_d$ ) values for  $K_p = 25$  by method 1

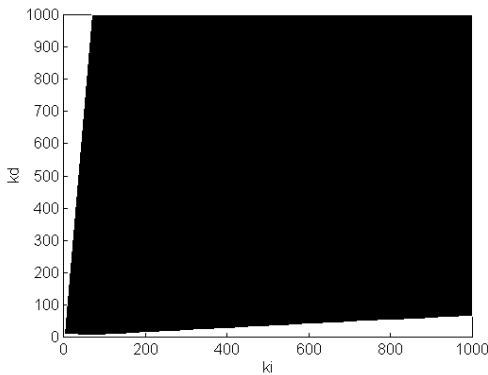


Fig. 7 The plane of ( $K_i, K_d$ ) values for  $K_p = 100$  by method 1

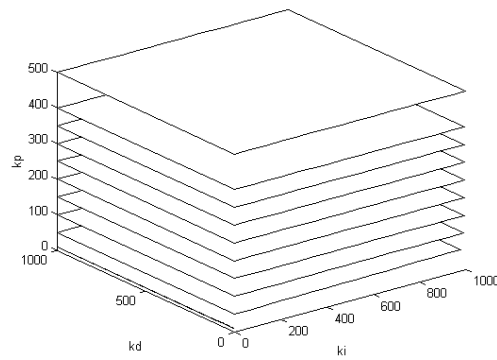


Fig.8 The stabilizing set of ( $K_p, K_i, K_d$ ) values by method 2

The stabilizing set of  $K_p$  from 20.608 to  $\infty$  is obtained by the method 1. The range of  $K_i$ ,  $K_d$  values for  $K_p$  varying from 20.608 to 500 is shown in fig. 5. The stabilizing set of  $K_p$  obtained by method 2 and method 3 are same and is from 9.82 to  $\infty$ . Figs 8 and 11 show the stabilizing set ( $K_i$ ,  $K_d$ ) values for  $K_p$  values from 9.82 to 500 which is obtained by adopting the method 2

and method 3 respectively. The plane of  $K_i, K_d$  values for a particular  $K_p$  is also drawn for method 1, 2 and 3. (Fig 6  $K_p=25$ , method 1, Fig 7  $K_p=100$ , method 1, Fig 9  $K_p=25$ , method 2, Fig 10  $K_p=100$ , method 2, Fig 12  $K_p=25$ , method 3, Fig 13  $K_p=100$ , method 3).

In method 4 we are assuming  $K_d$  value and finding out the stabilizing region of  $K_p, K_i$  as  $\omega$  varies from 0.01 to 22Hz. Fig. 14 shows the stabilizing set of  $K_p, K_i$  values for  $K_d$  from 1 to 1000. Figs 15 and 16 shows the region of stabilizing set of  $K_p, K_i$  obtained for  $K_d=1$  and 100 respectively. The region of stability is found out by evaluating  $J_f$ (here  $J_f$  is negative) and hence the right side of the stability boundary is the stable region, facing the direction in which  $\omega$  is increasing. This is shown shaded in figs 15 and 16. It is observed that the stabilizing region of  $K_p, K_i, K_d$  obtained by method 1 is less than the method 2, 3 and 4. This is mainly due to the interval operations involved in method 1. Results obtained by method 1 are conservative compared to other methods discussed in this paper.

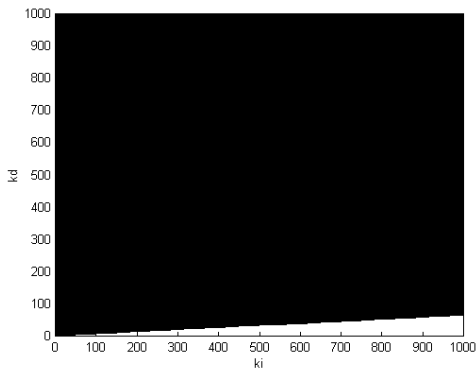


Fig. 9 The plane of (Ki, Kd) values for  $K_p = 25$  by method 2

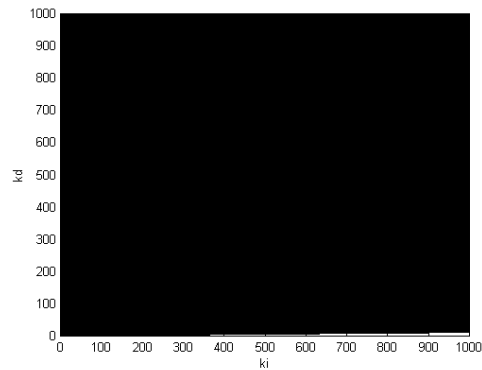


Fig. 10 The plane of (Ki, Kd) values for  $K_p = 100$  by method 2

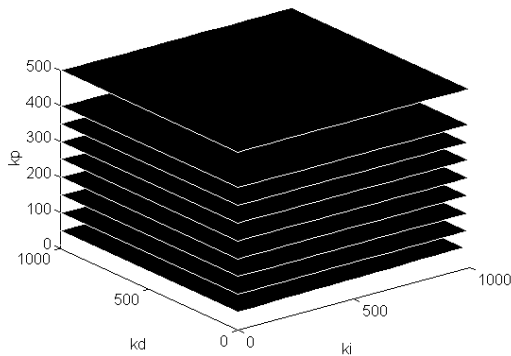


Fig. 11 The stabilizing set of (Kp, Ki, Kd) values by method 3

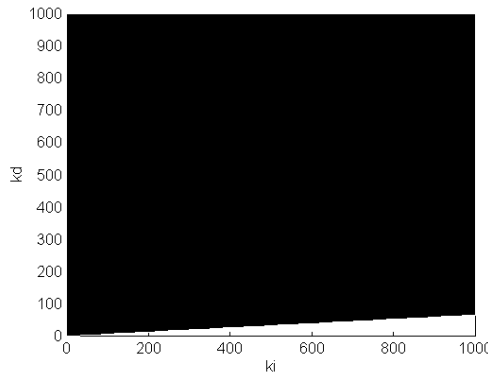


Fig. 12 The plane of (Ki, Kd) values for  $K_p = 25$  by method 3

From the class of stabilizing controllers obtained by all the methods we tried to design an optimal controller parameter ( $K_p, K_i, K_d$ ) by maximizing the fitness function  $J_f$

$$J_f = \frac{1}{1+J} \quad (26)$$

where  $J$  is the performance index given by  $J = \int_0^t e^2 dt$

The genetic algorithm based optimization technique [11] is used to obtain the optimal controller gains. The genetic operations applied were arithmetic crossover, uniform mutation and ranking selection. The GA was run for 25 generations with a population size of 80.

The initial conditions are chosen as  $x_1(0) = 0.0$  rad,  $x_2(0) = 0$ ,  $x_3(0) = 0$ . The desired angle is selected as  $0.524$  rad ( $30^\circ$ ). The range of controller gains  $K_i = [0.002, \infty]$  and  $K_d = [0.002, \infty]$  for  $K_p = 25$  are obtained using method 1 and the corresponding optimum controller gains  $K_i^* = 57.03$  and  $K_d^* = 15.11$  for  $K_p = 25$  are obtained by adopting genetic algorithm. The output and corresponding performance index value  $J_1$  ( is the performance index by method 1) is  $10.93$  are shown in fig. 17. Similarly graph 2, 3, 4 indicates the output response of the system for the optimal controller gains  $[(K_p = 25, K_i^* = 43.01, K_d^* = 5.23), (K_p = 25, K_i^* = 71.95, K_d^* = 9.18), (K_p = 25, K_i^* = 53.59, K_d^* = 7.24)]$  obtained from a search space of stabilizing controller parameters by method 2, 3, 4 respectively and the corresponding cost functions  $J_2 = 7.07, J_3 = 8.08, J_4 = 8.03$  are obtained.

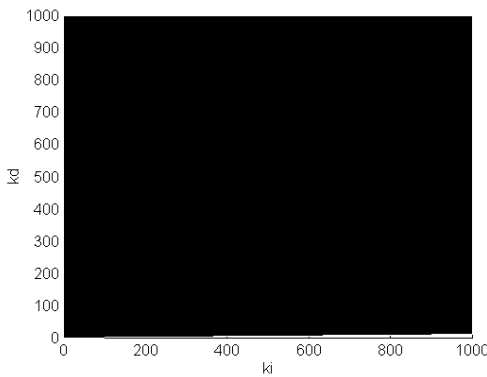


Fig. 13 The plane of (Ki, Kd) values for  $K_p = 100$  by method 3

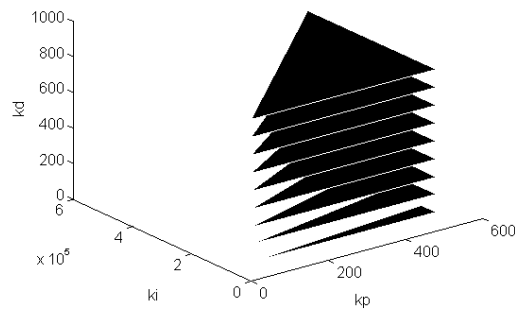


Fig. 14 The stabilizing set of (Kp, Ki, Kd) values by method 4

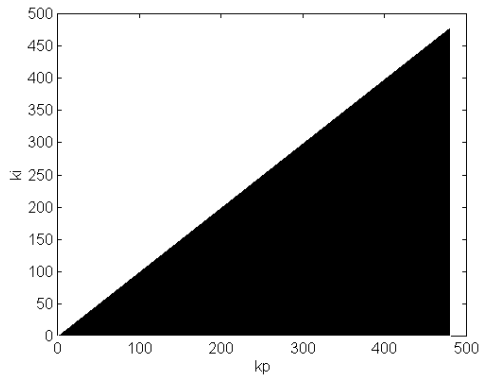


Fig. 15 The plane of (Kp, Ki) values for  $K_d = 1$  by method 4

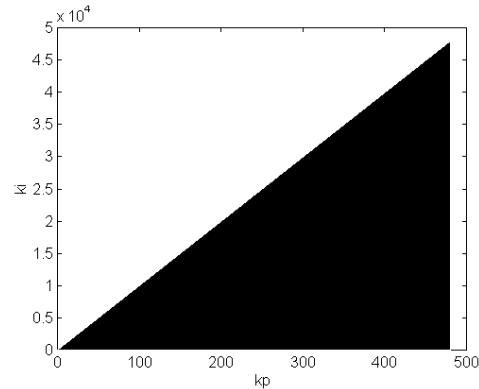


Fig. 16 The plane of (Kp, Ki) values for  $K_d = 100$  by method 4

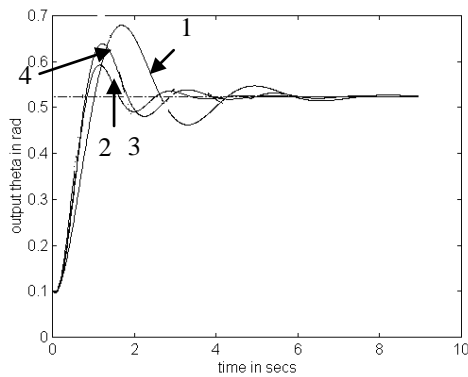


Fig. 17 Output  $\theta$  of the system

1  $K_p = 25, K_i^* = 57.03$  &  $K_d^* = 15.11$   
(method 1,  $K_i = [6.9, 500]$   $K_d = [9.9, 500]$ ),  
 $J_1 = 10.93$

2 and 3  $K_p = 25, K_i^* = 43.01$  &  $K_d^* = 5.23$   
(method 2,  $K_i [0.002, 500]$   $K_d [0.7, 500]$ ),  $J_2 = 7.70$

4  $K_p = 25, K_i^* = 53.59$  &  $K_d^* = 7.24$   
(method 4,  $K_i = [0.007, 500]$   $K_d = [1, 500]$ ),  
 $J_4 = 8.03$

We used the range of controller parameters ( $K_p = [9.82, \infty]$   $K_i = [0.002, \infty]$  and  $K_d = [0.002, \infty]$ ) obtained by method 3 which is also same as method 2 for obtaining an optimal controller parameter. Fig. 18 shows the output response of the system for fixed desired position  $\theta_d = 30^\circ$  with optimum value of controller gains [ $K_p^* = 488.31, K_i^* = 248.85, K_d^* = 22.80$ ]. Fig 19 shows the output of the system for time-varying desired position  $\theta_d = 1 - \cos(t)$  with optimum value of controller gains [ $K_p^* = 499.03, K_i^* = 493.39, K_d^* = 66.86$ ].

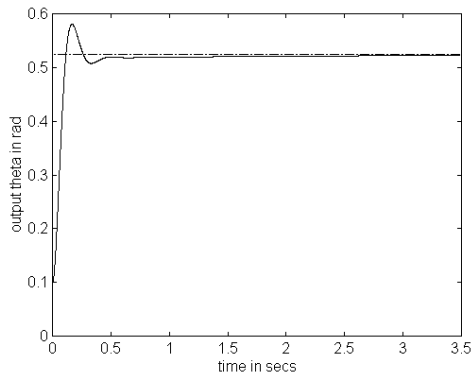


Fig. 18 Output  $\theta$  of the system for  $\theta_d = 0.524$  rad  $K_p^* = 488.31, K_i^* = 248.85, K_d^* = 22.80$   $J = 8.49$ .

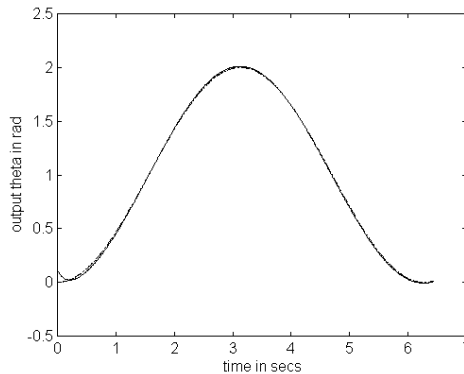


Fig. 19 Output  $\theta$  of the system for  $\theta_d = 1 - \cos(t)$   $K_p^* = 499.03, K_i^* = 493.39, K_d^* = 66.86, J = 0.14$ .

## 5. Conclusions

A class of stabilizing PID controllers for a single-link robot system is obtained by using different techniques. Concept of interval matrix, quadratic stability, stability boundary approach and Lyapunov function method are utilized to check the stability and subsequently the range of controller parameters are obtained using the procedure given in appendix I. The range of controllers obtained was used to obtain optimal controller parameters by employing genetic algorithm based optimization technique. Range of stabilizing controller parameters  $K_i$  and  $K_d$  for a fixed  $K_p$  obtained by using method 1 are conservative compared to other methods.

## Appendix I

Steps to obtain the range of controller parameters ( $K_p$ ,  $K_i$ ,  $K_d$ ).

Step (i) Any two values are assigned for  $K_p$  as 'a<sub>L</sub>' (lower bound) and 'a<sub>U</sub>' (upper bound).

Step (ii)  $K_i$  and  $K_d$  values are assigned arbitrarily from '-b' to 'b' and from '-c' to 'c' in steps of 1 respectively for the two values of  $K_p = 'a_L'$  and  $K_p = 'a_U'$ .

Step (iii) For these two set of controller gains ( $K_p = a_L$  &  $a_U$ ) we need to check the following condition depending upon the methods adopted

- Method 1 Solve the Lyapunov equation (6), taking  $Q_0$  as the identity matrix and obtain the  $P_0$  matrix. Check for positive definiteness of  $Q^1$  and  $Q^2$  obtained by equation (8).
- Method 2: Check for quadratic stability by computing the vertices of PLDI systems satisfying equation (9).
- Method 3: Assume  $Q$  as identity matrix, obtain the  $P$  matrix solving the Lyapunov equation,  $A^T P + PA = -Q$  for the system (4) with  $\theta = 90^\circ$  which is same as solving equations (14) - (19) with  $\theta = 90^\circ$ . Check for positive definiteness of matrix  $P$ .

If step (iii) is satisfied  $K_p$  value is retained as  $a_L$  or  $a_U$  and proceed to step(vi) else go to step (iv).

Step (iv) If we are not getting a  $K_p$  value for the above range of  $K_i$  and  $K_d$  values we change the  $K_i$  value to  $-r*b$  to  $r*b$  and  $K_d$  value to  $-r*c$  to  $r*c$  excluding the previously checked range of  $-b$  to  $b$  and  $-c$  to  $c$ . ( $r > 1$  is an integer quantity) Go to step (iii).

Step (v) If step (iii) is not satisfied after repeating step (iv),  $K_p$  is assigned new value of  $a_L/2$  or  $a_U/2$ .

Step (vi) To get the exact value of  $K_p$  we assign two new values of  $K_p$  as  $a_L - \Delta_a$  and  $a_U + \Delta_a$  where  $\Delta_a = 10^p$  and  $p$  is an integer. Numerical values of 'p' varies from positive to negative values (say  $p = \dots, -3, -2, -1, 0, 1, 2, 3, \dots$ ). For each  $\Delta_a$  starting from positive large values we repeat steps (ii) to (iv) until the step (iii) is

satisfied (ie till  $Q^1$  and  $Q^2$  matrices are negative definite for method 1, the systems defined by the corner matrices are quadratically stable for method 2, the  $P$  matrix is negative definite for method 3).

Step (vii) After obtaining  $K_p$  values the lower limit as well as upper limit we check whether  $K_p$  values exist from lower to upper limit. To do that steps ii to iv is repeated for  $K_p$  equal to lower value to  $K_p$  equal to upper value in small steps of length  $\Delta_{K_p}$ . If the interval matrix  $P$  is positive definite the value of  $K_p$  is stored in an array. If the difference between each element of the above array is greater than  $\Delta_{K_p}$  the range of  $K_p$  values is discontinuous. Steps (i) – (vii) are shown in flow-chart diagram.

Step (viii) Once  $K_p$  range is known the same steps (i) to (vi) are repeated to obtain the  $K_i$  values by arbitrarily assigning  $K_d$  values.

Step (ix) Once  $K_p$  and  $K_i$  values are known the same steps are repeated to get  $K_d$  values.

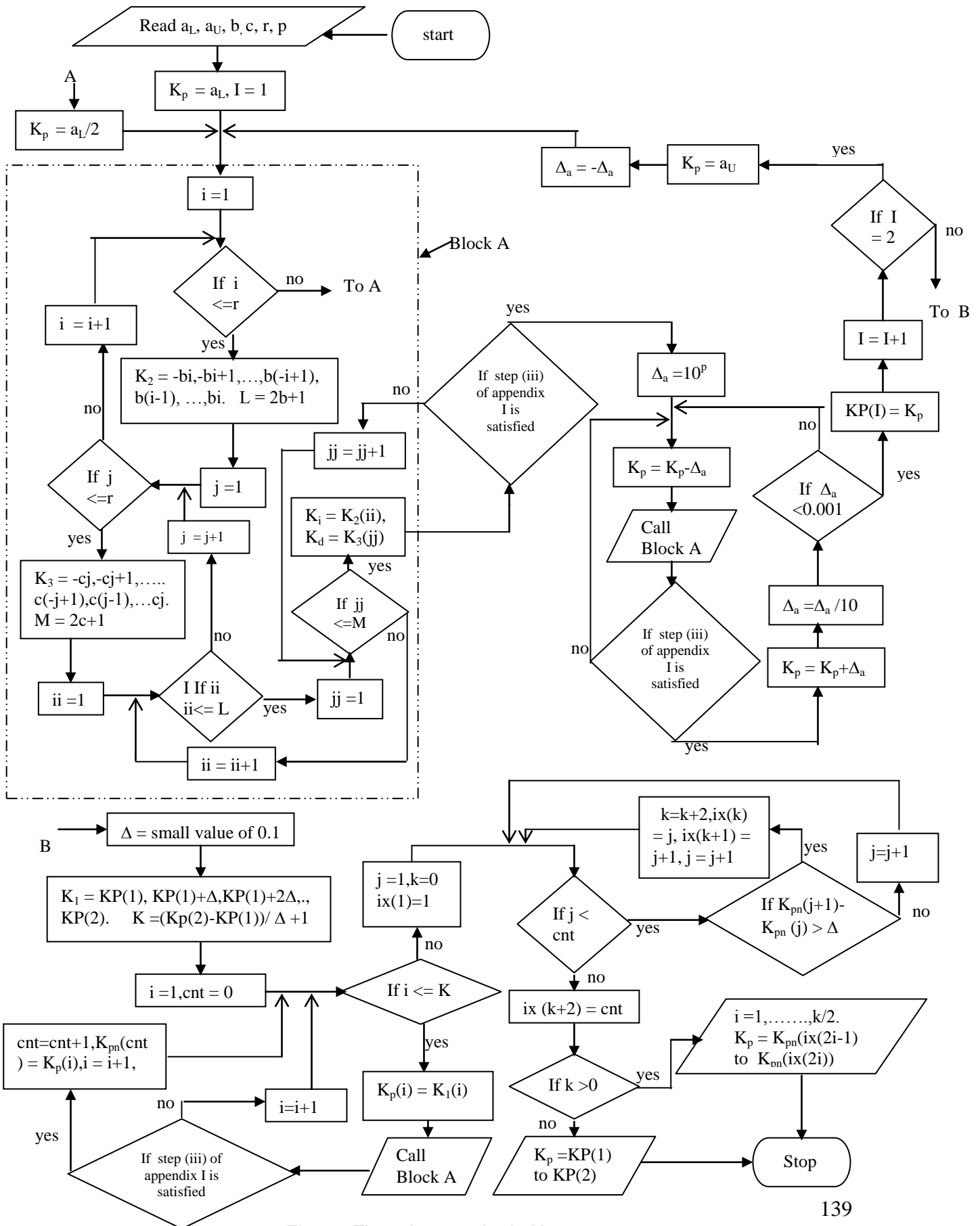


Fig. 20 Flow chart to obtain  $K_p$  range

**Appendix II : Using polytopes to describe time-varying systems [12]**

Let the strictly –proper linear time-varying system represented by the state variable realization

$$\dot{x}(t) = A(t)x(t) + B(t)u(t)$$

$$y(t) = C(t)x(t)$$

(A)

have k time-varying parameters  $q_i(t)$ , where  $q_i^- \leq q_i(t) \leq q_i^+$ ,  $i = 1, \dots, k$

The system represented by  $\{A(t), B(t), C(t)\}$  in (A) is a polytope of linear systems and can be defined by its vertices  $\{(A_1, B_1, C_1), (A_2, B_2, C_2), \dots, (A_L, B_L, C_L)\}$  where  $L = 2^k$ . For each time there is a set of L values  $\{p_j\}$ , such that

$$A = \sum_{j=1}^L p_j A_j, \quad B = \sum_{j=1}^L p_j B_j, \quad C = \sum_{j=1}^L p_j C_j, \quad \sum_{j=1}^L p_j = 1$$

and  $p_j \geq 0$  for  $j = 1, 2, \dots, L$ . The parameter space is a convex set, where the vertices are extreme values.

**Acknowledgement**

The authors would like to acknowledge the reviewers for their valuable comments.

**References**

[1] A. Datta, M. T. Ho, S. P. Battacharya, ‘Structure and Synthesis of PID Controllers’, Springer-Verlag, 2000.  
 [2] Z. Qu, D. M. Dawson, ‘Robust tracking Control of Robot Manipulators’, IEEE press New York, 1996.  
 [3] F. Garofalo, G. Celentano, L. Glielmo, ‘Stability Robustness of Interval Matrices Via Lyapunov Quadratic Forms’, IEEE Trans. On Automatic Control, vol. AC-38, No.2, Feb. 1993 pp 281-284.  
 [4] C. L. Jiang, ‘Sufficient condition for the asymptotic stability of interval matrices’, International Journal of Control vol.46, no. 5, 1987 pp 1803-1810.  
 [5] M. Mansour, ‘Sufficient condition for the asymptotic stability of interval matrices’, International Journal of Control vol. 47, no. 6, 1988, pp 1973-1974.  
 [6] S. Boyd, E. Feron, L. E. Ghaoui, V. Balakrishnan ‘Linear Matrix Inequalities in System and Control Theory’, Siam Philadelphia 1994.  
 [7] P. Gahinet, P. Apkarian, M. Chilali, ‘Affine parameter dependent Lyapunov approach functions and real parametric uncertainty’, IEEE Trans. On Automatic Control, vol. AC-41, Mar. 1996, pp 436-444.  
 [8] P. Gahinet, A. Nemirovski, A. J. Laub, M. Chilali, ‘LMI Control Toolbox for use with Matlab’, The Math works Inc May 1995.  
 [9] G. H. Lii, C. H. Chang, K. W. Han, ‘Analysis of Robust Control Systems using stability equations’ Journal of Control Systems and Technology, vol. 1, 1993, pp 83-89.  
 [10] D. D. Siljak, ‘Nonlinear Systems: The Parameter Analysis and Design’, John Wiley & Sons, N.Y (1969).  
 [11] D. E. Goldberg, ‘Genetic algorithms in search, optimization, and machine learning’, Addison Wesley, 1999.  
 [12] R. E. Benton Jr, D. Smith, ‘A non iterative LMI-based algorithm for robust static –output feedback stabilization’, Int. J. of Control 1999, vol.72, no. 14, 1322-1330.  
 [13] Yun Li, K. H. Ang, G. C. Y. Chong, PID Control System Analysis and Design- problems remedies and future directions, IEEE Control system magazine, Feb 2006, pp. 32-41.  
 [14] H. Oya, K. Hagino, ‘Trajectory based design of robust non fragile controllers for uncertain linear systems’, 32 nd Annual Conference on Industrial Electronics, 2007, pp.294-300.  
 [15] E. Fridman, U. Shaked, ‘Parameter dependent stability and Stabilization of uncertain time delay systems, IEEE Trans on Automatic Control, 2003, pp.861-866.  
 [16] Y. He, M. Wu, J. H. She, ‘Parameter dependent Lyapunov functional for stability of time delay systems with polytopic –type uncertainties’, IEEE Trans on Automatic Control, vol. 49, 2004, pp. 828-832.  
 [17] T. Hu, Teel A. R., Zaccarian L., ‘Stability and Performance of Saturated systems via quadratic and non-quadratic lyapunov function’, IEEE Trans on Automatic Control, vol. 49, 2004, pp.828-832.

- [18] Qing-Guo Wang, a, , Yong Hea, Zhen Yea, Chong Lina and Chang Chieh Hanga, 'On loop phase margins of multivariable control systems, Journal of process Control, vol.18, issue 2, Feb 2008, pp.202-211.
- [19] Zhen Ye, Qing-Guo Wang and Chang Chieh Hang, Frequency Domain Approach to Computing Loop Phase Margins of Multivariable Systems, Ind. Eng. Chem. Res., 2008, 47 (13), pp 4418–4424.
- [20] Qian Sang; Gang Tao, IEEE Transactions on Automatic Control, Volume: 55 Issue:1, Jan 2010, pp.104 – 115.
- [21] Ying J. Huang, Yuan J Wang, Robust PID Tuning strategy for uncertain plants based on the Kharitonov theorem, ISA transactions, 39,2000, pp. 419-431.

## Authors



**Dr. Leena G.** has B-Tech in Electrical and Electronics Engg. and M-Tech in Control Systems from Kerala University in 1991 and 1995 respectively. She completed her PhD in 2007 from Indian Institute of Technology, Kharagpur, India. She had over 15 years of teaching experience and presently she is heading the Electrical and Electronics Department of Manav Rachna International University, Faridabad, India. Her areas of interest are nonlinear system, decentralized control, sliding mode control etc.



**Kanti Bhushan Datta**, Ph.D., D.Sc., FNAE, served for 19 years (1982–2001) in the Department of Electrical Engineering, Indian Institute of Technology Kharagpur where he remained Professor from 1985 to 2001. His another major tenure for 17 years (1965–1982) had been in the Department of Applied Physics, University of Calcutta. His field of interest in multivariable control systems, robust control and  $H_2/H_\infty$  control theory.



**Dr. G Ray** is Phd from Indian Institute of Technology Delhi, India. He is currently a Professor in the Department of Electrical Engineering, Indian Institute of Technology, Kharagpur India. His research interests are in intelligent control, robust stabilization, time delay system, decentralized control and state estimation.

